


RESEARCH ARTICLE

Insertion of the Fe_B cofactor in cNORs lacking metal inserting chaperones

Sofia Appelgren and Pia Ädelroth 

Department of Biochemistry and Biophysics, Stockholm University, Sweden

Correspondence

P. Ädelroth, Department of Biochemistry and Biophysics, Stockholm University, SE-106 91 Stockholm, Sweden
Tel: +46 8 164183
E-mail: pia.adelroth@dbb.su.se

(Received 27 June 2024, revised 26 November 2024, accepted 16 January 2025, available online 10 February 2025)

doi:10.1002/1873-3468.70007

Edited by Seema Mattoo

Cytochrome *c*-dependent nitric oxide reductase (cNOR) catalyzes the reduction of NO into nitrous oxide (N₂O), a strong greenhouse gas released from denitrifying microorganisms. The cNOR active site holds an essential non-heme iron, Fe_B, inserted using the chaperone complex NorQD. However, in *Thermus thermophilus*, the cNOR (TtcNOR) cluster lacks the *norQD* genes. Here we investigated Fe_B insertion into TtcNOR and characterized and compared TtcNOR expressed in *Escherichia coli* to that natively produced. We show that Fe_B is present in the natively produced TtcNOR only. Analysis of cNOR operon sequences suggests that a hydrophilic K-pathway analogue is present in cNORs that do not rely on NorQD for iron insertion. We discuss the implications of our data for the evolution of the NOR family.

Keywords: evolution; iron; K-pathway; nitric oxide reductase; norQ; *Thermus thermophilus*

Denitrification, i.e., respiration using nitrate as electron acceptor, is performed by microorganisms inhabiting soils and marine environments where nitrate is present. The process involves a stepwise reduction of nitrate into dinitrogen, $\text{NO}_3^- \rightarrow \text{NO}_2^- \rightarrow \text{NO} \rightarrow \text{N}_2\text{O} \rightarrow \text{N}_2$, and each reaction is catalyzed by one (soluble or membrane-bound) enzyme. Not all denitrifying organisms have the full set of necessary enzymes to perform complete denitrification and will release intermediates (instead of N₂) into the environment. Nitrous oxide (N₂O) is a potent greenhouse and ozone layer depleting gas [1], released by microbes performing incomplete denitrification. The Great Boiling Spring in the US is an example of a habitat with large emissions of N₂O, in part due to bacteria of the *Thermus* genus doing incomplete denitrification [2]. The reduction of nitric oxide into nitrous oxide ($2\text{NO} + 2\text{e}^- + 2\text{H}^+ \rightarrow \text{N}_2\text{O} + \text{H}_2\text{O}$) is catalyzed by the membrane protein

nitric oxide reductase (NOR), which is a member of the superfamily of heme-copper oxidases (HCuO), and thus shares evolutionary history with its O₂-reducing members. NORs are categorized based on their electron donor, which can be for example cytochrome *c* (cytochrome *c*-dependent nitric oxide reductase, cNOR) or quinol (quinol-dependent nitric oxide reductase, qNOR), and these two types of characterized NORs are related to the C-type O₂-reducing HCuOs [3]. Recently, also sequences for other suggested NORs, related to the B-type O₂-reducing HCuOs were discovered [4]. cNOR is a heterodimer, consisting of the two subunits NorC and NorB, while qNOR consists of the single subunit NorZ, holding an extracellular domain similar to NorC. Thus, *norZ* is presumably the result of a gene fusion of *norB* and *norC*. cNOR has one heme *c*, located in the NorC subunit, and two hemes *b*, located in the NorB subunit, of which one is

Abbreviations

AAA+ ATPase, ATPases associated with diverse cellular activities; Asc, ascorbate; cNOR, cytochrome *c*-dependent nitric oxide reductase; DDM, *n*-dodecyl-β-D-maltoside; GDN, glyco-diosgenin; HCuO, heme-copper oxidase; MCS, multiple cloning site; PacNOR, *Pseudomonas aeruginosa*; PdcNOR, *Paracoccus denitrificans* cNOR; PMS, phenylmethanesulfonic acid; TMPD, *N,N,N,N*-tetramethyl-*p*-phenylenediamine; TtcNOR, *Thermus thermophilus* cNOR; VWA, Von Willebrand factor A; βOG, *n*-octyl-β-D-glucoside.

found in the active site, accompanied by a non-heme iron (Fe_B). qNOR has an identical setup of ligands, except lacking the heme *c*. The heme *b*₃ – Fe_B binuclear active site of NOR is homologous to the heme *a*₃ – Cu_B active site of O₂-reducing HCuOs and the non-heme metal is probably adapted to the different substrates, NO or O₂. The mechanism of N₂O formation in NORs is not fully understood, and still highly debated [5–12], but the Fe_B is essential in all scenarios. The most studied cNORs originate from bacteria in the Pseudomonadota phylum, such as *Pseudomonas stutzeri* [13,14], *Paracoccus denitrificans* [15,16], *Halomonas halodenitrificans* [17,18], *Roseobacter denitrificans* [19–21] and *Pseudomonas aeruginosa* [9,22]. For the latter two there are high-resolution 3D structures available [20,22]. In contrast to cytochrome *c* oxidase, the cNORs studied so far are not electrogenic as they acquire substrate protons from the periplasm [5,23] and don't pump any protons. qNORs do have a putative proton pathway from the cytosol to the active site, spatially homologous to the K-pathway of cytochrome *c* oxidase, and could therefore be electrogenic [24,25]. For a review of the structure and function of cNORs and qNORs, see [26]. The most studied cNORs have gene clusters containing six genes: *norC* and *norB*, encoding the two structural subunits, followed by *norQ* and *norD*, encoding soluble chaperone proteins NorQ and NorD, essential for insertion of Fe_B into the active site [27], and *norE* and *norF*, encoding putative small membrane proteins of unclear function. The two metal-inserting chaperone proteins NorQ, a AAA+ ATPase (ATPases Associated with diverse cellular Activities), and NorD, a Von Willebrand domain factor type A (VWA) domain containing protein, form a NorQD complex, suggested to interact with the Fe_B-less cNOR to activate it. NorD holds a metal ion adhesion site (MIDAS), consisting of five residues coordinating a divalent metal ion, with the 6th ligand assumed to be supplied by acidic surface residues on the cytoplasmic side of NorB. The chaperone complex presumably causes conformational changes in cNOR, fueled by ATP hydrolysis by NorQ, which enables iron to access the active site [28].

However, the cNOR gene clusters of bacteria in the *Thermus* genus are shorter, consisting of only three genes: *norC* and *norB*, homologs to the structural genes described above, and a *norH* gene, with no homologs in the previously characterized cNORs [29]. Hence, the *Thermus* cNOR lacks chaperones for the insertion of Fe_B into the cNOR enzyme. This is similar to gene clusters for qNOR, which can incorporate the non-heme iron without assistance from chaperone proteins [24]. Interestingly, both qNOR and *Thermus*

thermophilus cNOR (*TtcNOR*) lack the previously mentioned surface residues suggested to bind the NorQD complex [28]. The *norH* gene encodes NorH, a third cNOR subunit, suggested to be structural and important, but not essential, for NO reduction *in vivo* [30]. As NorH is found in cNOR gene clusters of several thermophilic bacteria, it is also possibly of importance for thermostability [30].

Thermus thermophilus genes for nitrate respiration are found on a nitrate respiratory conjugation element (NCE). The NCE consists of four gene clusters encoding a nitrate reductase, nitrate/nitrite transporters, an NADH dehydrogenase and regulatory proteins. This element, and hence the ability to respire nitrate, is common in *Thermus* species, and is easily transferred by lateral conjugation [31,32]. Less common is the ability to respire nitrite. This requires an additional *nir-nor* cluster, encoding nitrite reductase (Nir) and NOR, also transferrable by lateral gene transfer. HB27, a common, strictly aerobic laboratory strain of *T. thermophilus*, was shown to denitrify when transformed with the NCE and *nir-nor* cluster from the denitrifying strain PRQ25. The resulting strain is denoted HB27d [29]. The denitrification genes are not found in the *Thermus* genome, but on a megaplasmid. For a review on denitrification in *T. thermophilus* and the lateral gene transfer thereof, see Ref. [33].

Thermus thermophilus cNOR has previously been expressed homologously in *T. thermophilus*, transformed with the *TtcNOR* operon on an engineered vector, and heterologously in *Escherichia coli*, and characterized by activity measurements and mutagenesis studies in the heterologous system. *TtcNOR* has a low NO-reducing activity with a *k*_{cat} of 2.5–10 e[−]·min^{−1} [34], whereas for example cNOR from *Paracoccus denitrificans* (*PdcNOR*) has an activity of 40–70 e[−]·s^{−1} [35] and *Pseudomonas aeruginosa* cNOR (*PacNOR*) of 7 e[−]·s^{−1} [22]. The activity of *TtcNOR* can also be compared to the capability of the O₂-reducing *ba*₃ and *caa*₃ HCuOs in *T. thermophilus* to reduce NO at rates of 3 and 32 e[−]·min^{−1} respectively [36]. Furthermore, the *TtcNOR* does not show any signs of the characteristic cNOR substrate inhibition pattern [34]. Mutagenesis studies of *TtcNOR* expressed in *E. coli* showed that mutations of conserved residues for Fe_B binding barely impacted its activity, nor the iron content [34].

Intrigued by the lack of metal-inserting chaperones and the low activity of the purified *TtcNOR*, we wanted to investigate if there was a relation between these two properties. We expressed *TtcNOR* both natively in *T. thermophilus* HB27d from the NCE-*nir-nor* clusters and in *E. coli*, and compared the

two preparations with regards to non-heme iron content, catalytic activity and ligand-binding properties. We also compared the activity of *TtcNOR* in different detergents to its activity in membranes. Electron donors used in previous studies of *TtcNOR* include TMPD (*N,N,N',N'*-tetramethyl-*p*-phenylenediamine), PMS (phenylmethanesulfonic acid) and *T. thermophilus* cyt *c*₅₅₂, suggested to be the native electron donor. The *nir* gene cluster of *T. thermophilus* encodes an additional small soluble cyt *c*, *nirM* [29]. Here, we expressed and purified NirM and tested it as electron donor for *TtcNOR*. Furthermore, we analyzed available sequence data for the occurrence of cNORs without *norQD* in the cluster and investigated if there are sequence differences between cNORs that do and do not need/use metal-inserting chaperones.

Methods

Strains and molecular biology

Production of natively expressed *TtcNOR* was done in the *T. thermophilus* strain HB27d [29]. HB27d was genetically modified with a C-terminal 6× his-tag on *norH* in the NCE-*nir*-*nor* denitrification gene cluster, using a suicide plasmid, and a kanamycin resistance gene [30]. The resulting strain is in this work denoted HB27d-*cNOR*. The HB27d strain with a knocked out *norB* gene [30], denoted HB27d-Δ*norB*, was used for negative controls.

For expression of *TtcNOR* in *E. coli*, the gene cluster was cloned from the pMK-*cNOR* vector [34] using primers in Table S1, and inserted into the pET-Duet1 vector MCS2, with the S-tag exchanged for a strep-tag, described in Ref. [28], resulting in a vector denoted pET-Duet1-*TtcNOR*. MCS1 was left empty. In this construct, *TtcNOR* was double tagged, with one N-terminal 8× his-tag on *norB*, originating from the pMK-*cNOR* vector, and a C-terminal strep-tag on *norH*, from the pET-Duet1 backbone.

The gene *nirM* was ordered from Genscript in a pET21a vector with a modified signaling peptide similar to the one used for *TtcNOR* in Ref. [37] and a C-terminal strep-tag. The gene was codon optimized for *E. coli* (sequence in Fig. S1). For expression of *TtcNOR*, a pET16b vector encoding the N-terminally his-tagged *TtcNOR* was used, based on the vector from [38].

Growing and purification

Thermus thermophilus HB27d-*cNOR* was grown anaerobically in *Thermus* LB (8 g·L⁻¹ peptone from meat, 4 g·L⁻¹ yeast extract, 3 g·L⁻¹ NaCl, 2.3 g·L⁻¹ KNO₃, pH 7.5) at 60 °C with 60 r.p.m. shaking for 24–48 h. Purification was done as for *PdcNOR* described in Ref. [27]. Briefly, the cells were harvested and suspended in buffer (100 mM

TRIS/HCl, pH 7.6, 50 mM KCl, supplemented with DNase I and 1 tablet complete EDTA-free protease inhibitor cocktail) and crushed at 25 kpsi, followed by ultracentrifugation to isolate the membranes. Pelleted membranes were solubilized in 1% DDM (*n*-dodecyl-β-D-maltoside), followed by ultracentrifugation. The solubilized membranes were mixed with Ni-NTA gel for 1 h and then applied on a column. The column was washed with buffer (50 mM imidazole, 50 mM TRIS/HCl, pH 7.6, 200 mM KCl, 0.05% DDM) and the protein was eluted with the same buffer containing 250 mM imidazole. The eluted protein was concentrated up to approximately 10 μM and the concentration of cNOR was estimated using $\epsilon_{410,ox} = 311 \text{ mM}^{-1}\cdot\text{cm}^{-1}$. Solubilization with GDN (glyco-diosgenin) instead of DDM was done similarly. From now on, 'purified *TtcNOR*' refers to the enzyme solubilized in DDM, unless stated otherwise. *T. thermophilus* HB27d-*cNOR* and HB27d-Δ*norB* for activity measurements in membranes were grown, crushed and ultracentrifuged in the same way as membranes used for protein purification.

For heterologous expression of *TtcNOR* in *E. coli*, the *E. coli* strain BL21 DE3 was transformed with the pET-Duet1-*TtcNOR* vector and the pEC86 vector, enabling heme *c* production in *E. coli* [39]. The pRARE vector used previously [34] was found non-essential for expression and not used. The cells were grown in TB media without induction [40], at 37 °C, 180 r.p.m., until OD₆₀₀ reached 0.5. The temperature was then first lowered to 30 °C for 5 h, followed by a 5 h long period of 18 °C without shaking. Then, the temperature was again raised to 30 °C and shaking at 180 r.p.m. for 6 h before harvesting, as previously for *PdcNOR* expression in *E. coli* [41]. Resuspension, crushing, solubilization, and ultracentrifugation was done as for natively expressed *TtcNOR*, described above. Since *TtcNOR* expressed in *E. coli* was tagged with both a his-tag on *NorB* and a strep-tag on *NorH*, the solubilized membranes were divided in two parts, one was purified on the Ni-NTA column as described above. The other was applied to a strep column, washed with buffer (50 mM TRIS/HCl, pH 7.6, 200 mM KCl, 0.05% DDM) and eluted with the same buffer containing 10 mM desthiobiotin. Eluted protein was concentrated and cNOR concentration was determined as described above.

Both cyt *c*₅₅₂ and NirM were expressed heterologously in the *E. coli* strain BL21 DE3 holding the pEC86 vector. The cells were grown in TB media, supplemented with 10 mM MgSO₄ and 200 μM FeSO₄ at 37 °C, shaking at 180 r.p.m. When cells reached an OD₆₀₀ of 2, protein expression was induced with 0.5 mM IPTG and the temperature was lowered to 30 °C and the cells were grown for another 16 h. Upon harvesting, cells were resuspended in buffer (50 mM HEPES-NaOH, pH 8.0, 0.05% Triton X-100, 0.5 M NaCl supplemented with DNase I and 1 tablet complete EDTA-free protease inhibitor cocktail). Cells were crushed and ultracentrifuged as described above. Supernatants were

collected and incubated at 50 °C for 15 min, followed by centrifugation. The supernatant was collected and applied to either Ni-NTA column (cyt *c*₅₅₂) or strep resin column (NirM). For purification of his-tagged cyt *c*₅₅₂, the column was first washed with buffer (10 mM HEPES, pH 8.0, 30 mM imidazole; 0.05% Triton X-100, 1 M NaCl) followed by a wash with the same buffer without detergent. Cyt *c*₅₅₂ was eluted with 10 mM HEPES pH 8.0, 250 mM imidazole, 1 M NaCl. For purification of strep-tagged NirM, the column was washed with buffer (10 mM HEPES pH 8.0, 1 M NaCl) and eluted with the same buffer containing 10 mM desthiobiotin. Both cytochromes were put on dialysis against 5 mM HEPES, pH 8, 400 mM NaCl overnight. The concentration of the cytochromes was estimated using $\epsilon_{552,\text{red-ox}} = 14.4 \text{ mM}^{-1} \cdot \text{cm}^{-1}$ [37].

Mass-spectrometry

Preparations of purified *TtcNOR* expressed natively and solubilized in DDM or GDN, and *TtcNOR* expressed in *E. coli* solubilized in DDM were trypsin cleaved and the fragments were analyzed by mass-spectrometry, performed by the SciLifeLab Mass Spectrometry Facility at Uppsala University using nano-LC-MS/MS.

Non-heme iron measurement

The content of non-heme iron was measured using the ferene method [42,43]. In the ferene method, the protein and its heme groups are precipitated, whereas the non-heme iron unbinds from the protein and forms a colored complex with ferene. Thus, the Fe_B content can be measured spectroscopically, without interference from heme iron. *cNOR* was diluted to 7 μM in 60 μL buffer (50 mM HEPES, pH 7.5, 50 mM KCl, 0.05% DDM). HCl 37% (6 μL) was added and the enzyme was left to precipitate for 5 min, followed by centrifugation. Then, 100 μL of 3 M sodium acetate and 10 μL 1 M ascorbic acid (pH 6) was added to the supernatant and the absorbance at 593 nm was recorded. Then, 10 μL of 3 mM ferene was added and the sample was left in the dark for 5 min, and absorption at 593 nm was again recorded. The difference in 593 absorbance before and after ferene addition was used to determine the content of non-heme iron, using $\epsilon_{593} = 35.5 \text{ mM}^{-1} \cdot \text{cm}^{-1}$ [42].

NO activity measurements

The activity of purified *TtcNOR* expressed natively and heterologously in *E. coli* was determined using an NO electrode (World Precision Instruments). *cNOR* was diluted to 0.25 μM in 50 mM HEPES, pH 7.5, 50 mM KCl, 0.05% DDM, with 30 mM glucose and 10 $\text{U} \cdot \text{L}^{-1}$ catalase. The chamber was closed, and glucose oxidase was added to a concentration of 1 $\text{U} \cdot \text{mL}^{-1}$. Once the system was depleted

of O₂, NO was added from a saturated (2 mM) solution in five steps of 10 μM , up to 50 μM . Electron donors were added, and NO consumption could be followed over time. Activity was calculated at NO concentrations between 50 and 10 μM . The measurements were repeated without enzyme, and the rate of NO consumption without *cNOR* added was subtracted from the calculated rates. The measurements were performed at room temperature and in duplicates.

To determine the NO-reducing activity in membranes, 40 mg of the pelleted membranes were suspended in 1 mL of buffer (50 mM HEPES, pH 7.5, 50 mM KCl) supplemented with 30 mM glucose and 10 $\text{U} \cdot \text{L}^{-1}$ catalase. The measurements were performed as described for the purified proteins. Measurement was also done on the same mass of membranes from HB27d- ΔnorB as control.

CO recombination

CO recombination to *TtcNOR* was followed using flash photolysis on a rapid kinetic setup (Applied Photophysics, Leatherhead, UK), essentially as described previously [44]. Briefly, the protein was diluted to 1 μM in buffer (50 mM HEPES, pH 7.5, 50 mM KCl, 0.05% DDM) in a modified Thunberg cuvette. The atmosphere was exchanged for N₂ on a vacuum line and the protein was reduced using ascorbate, PMS and dithionite, whereafter the atmosphere was changed to 100% CO. CO was dissociated from heme *b*₃ using a 10-ns laser flash (Quantel) and recombination was studied using optical spectroscopy at selected wavelengths (415–435 nm). The atmosphere in the cuvette was changed to 20% CO and 80% N₂, and the experiment was repeated. The obtained kinetic traces were averaged and analyzed as described previously.

Sequence analysis

To investigate the occurrence of *cNOR* operons without *norQD*, we collected the *NorB* sequences analyzed in Ref. [45] from the NCBI database [46]. If a MoxR AAA+ ATPase and a VWA domain protein were encoded in proximity to *norC* and *norB* genes, the *cNOR* was classified as having *NorQD* chaperones. If not, the *cNOR* was classified as lacking *NorQD* chaperones. Alignments were done using CLUSTAL OMEGA [47] and ESPRIT 3.0 [48]. ALPHAFOLD-MULTIMER [49,50] in Google Colab [51] via CHIMERA-X [52] was used to model *TtcNOR* from the *NorC*, *NorB* and *NorH* sequences.

Results

Characterization of produced proteins

We expressed and purified the *TtcNOR* both natively and heterologously in *E. coli*. The yield of

natively expressed *TtcNOR* solubilized in DDM was low (Table S2). The enzyme was eluted in its oxidized state, and dithionite reduced spectra show characteristic cNOR heme peaks (Fig. 1). We also used the milder detergent GDN, known to stabilize supercomplexes [53]. When solubilizing membranes in GDN, the overall yield was lower and NorC was less prominent, both as seen on SDS/PAGE gel and in spectra (Fig. 1). The yield of *TtcNOR* expressed in *E. coli* was high when pulling on his-tagged NorB, but the enzyme came off the column more reduced and the heme *c* peak was shifted from 552 to 553 nm, compared to the natively expressed *TtcNOR*. Purification using the strep-tag on NorH from *E. coli* gave a very low yield and an unstable cNOR, precipitating quickly upon reduction with dithionite. The SDS/PAGE gels of natively expressed *TtcNOR* purified in DDM show bands for the three subunits NorB, NorC, and NorH plus several high MW bands, of which some dissociated into NorB and NorC bands upon boiling the SDS/PAGE sample. Similar behavior was observed for

the sample solubilized in GDN, although the overall purity was lower. For *TtcNOR* expressed in *E. coli*, strong bands indicating NorB and NorC were observed and also bands of higher MW. Upon boiling, the NorB band (as well as high MW bands), disappeared, probably due to aggregation. This is similar to *PdcNOR* when expressed in *E. coli*. Whether NorH is present in *TtcNOR* expressed in *E. coli* is not clear.

We also expressed the putative *TtcNOR* electron donors cyt *c*₅₅₂ and NirM in *E. coli*. Yields, purities, and peaks of cyt *c*₅₅₂ and NirM are found in Table S2. In the reduced spectra (Fig. S2), cyt *c*₅₅₂ showed a broad peak at 555 nm in the alpha region, indicating co-purification of the dimeric *c*₅₅₇, consisting of two covalently bound cyt *c*₅₅₂ as observed previously [37].

Mass-spectrometry

Preparations of *TtcNOR* expressed natively and solubilized in DDM or in the milder detergent GDN, and *TtcNOR* expressed in *E. coli* were analyzed using

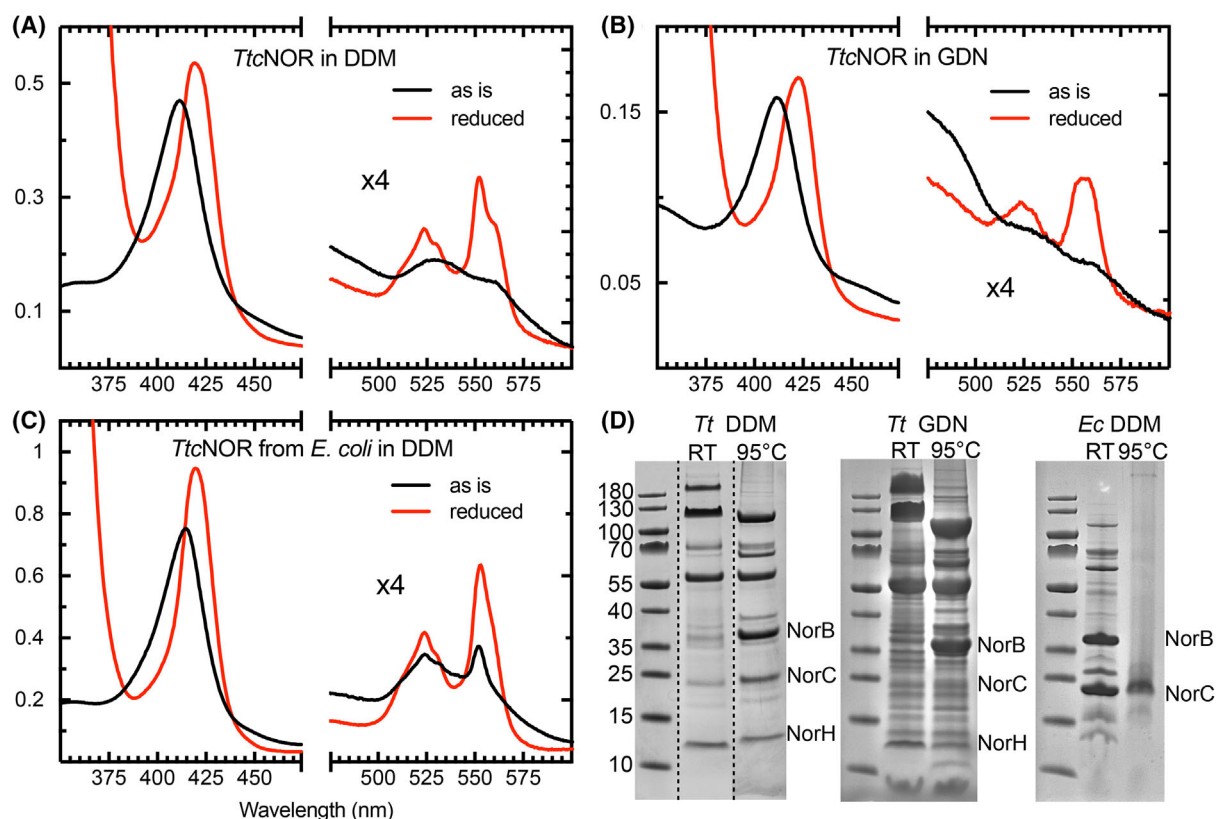


Fig. 1. Spectra of (A) *TtcNOR* expressed natively and solubilized in DDM, (B) *TtcNOR* expressed natively and solubilized in GDN, (C) *TtcNOR* expressed in *Escherichia coli* and solubilized in DDM. (D) SDS/PAGE gels of the purified *TtcNOR*s. First lane: Ladder. Second lane: Protein after incubation in LDS buffer for 10 min at RT. Third lane: Protein after incubation in LDS buffer for 10 min at 95 °C. The dashed lines indicate that the two lanes have been assembled from different parts of the same gel, see original gel in Fig. S3.

Table 1. Non-heme iron content in different preparations of *TtcNOR* and *PdcNOR*. Mean and standard deviation of two measurements. *Ec*, *Escherichia coli*; *Tt*, *Thermus thermophilus*.

Sample	cNOR (nmol)	Fe _B (nmol)	Fe _B /cNOR
<i>TtcNOR</i> in <i>Tt</i>	0.28	0.35 ± 0.0008	1.25 ± 0.003
<i>TtcNOR</i> in <i>Ec</i>	0.34	0.04 ± 0.01	0.12 ± 0.03
<i>PdcNOR</i> in <i>Ec</i> ^a	0.28	0.26 ± 0.01	0.95 ± 0.05
<i>PdcNOR</i> Δ <i>norQD</i> in <i>Ec</i> ^a	0.28	0.07 ± 0.004	0.25 ± 0.02

^aThe data for *PdcNOR* with and without chaperones was similar to that published previously [27].

mass-spectrometry, to investigate putative co-purified proteins. In all samples, NorB and NorC subunits were identified, however, NorH was not, probably due to its hydrophobicity. The five highest scoring co-purified proteins, and scoring results for NorB and NorC, are presented in Table S3. In the native DDM sample, nitrite reductase was identified with a low score. No other known proteins involved in denitrification, except cNOR, were identified.

Non-heme iron

Non-heme iron measurements (Table 1) on *TtcNOR* expressed natively show that the enzyme has a non-heme iron content of 1.25 ± 0.003 ($n = 2$) Fe_B per enzyme, similar to *PdcNOR* expressed in *E. coli* [27,28]. Thus, there is no doubt that cNOR expressed natively contains the non-heme iron. However, *TtcNOR* expressed in *E. coli* contains much less non-heme iron, 0.12 ± 0.03 ($n = 2$) Fe_B per enzyme. This

amount of non-heme iron is comparable to *PdcNOR* expressed in *E. coli* without the non-heme iron inserting chaperones present [27,28].

Activity of purified cNOR with different electron donors

NO-reducing activity of *TtcNOR* expressed natively was measured at room temperature with different electron donors. Our data (Fig. 2 and Table 2) is consistent with the very low numbers reported previously for cNOR expressed from the pMK-cNOR vector in *T. thermophilus* and heterologously in *E. coli* [34]. No increase in activity was observed with either cyt *c*₅₅₂ nor NirM. The *TtcNOR* expressed in *E. coli* in this work had similar activity, although lacking non-heme iron. We also note that no substrate inhibition is observed at higher [NO] (see Discussion).

Activity of cNOR in membranes

NO reduction was also measured in the HB27d-cNOR membranes, with TMPD and ascorbate or PMS and ascorbate as electron donors (Table 3). Membranes from HB27d-Δ*norB* were used as control for possible prevalence of other NO-reducing enzymes. The activity in HB27d-cNOR membranes (with the slope in HB27d-Δ*norB* membranes subtracted) was ~130 nM NO·min⁻¹·mg⁻¹ membranes. In the membranes, we can for the first time observe substrate inhibition of *TtcNOR*, with a clear increase in activity at low [NO], compared to the HB27d-Δ*norB* control (Fig. 2). However, determination of the cNOR

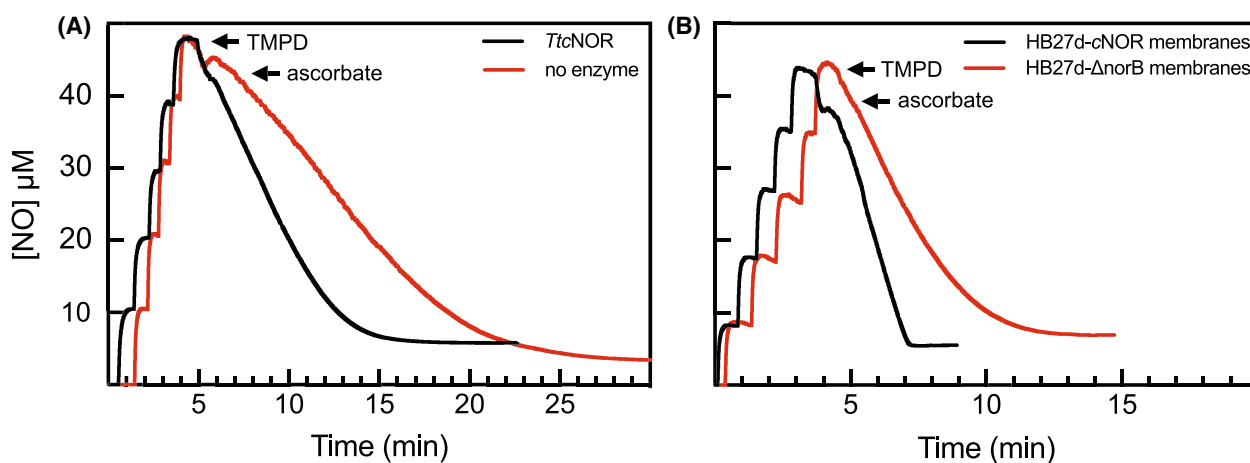


Fig. 2. Examples of activity traces. (A) Purified *TtcNOR* (black) and control experiment without enzyme (red). (B) Membranes from the denitrifying strain HB27d-cNOR (black) and membranes from the strain HB27d with *norB* knocked out. Protein or membranes were added prior to oxygen depletion (at $t < 0$). NO was added ($5 \times 10 \mu\text{M}$) at $t \sim 0$, after which the electron donors were added as indicated.

concentration in membranes is not straight-forward. Assuming that all cNOR in the membranes could be purified gives a $k_{\text{cat}} = 600 \text{ e}^- \cdot \text{min}^{-1}$ for membrane-bound cNOR. Normalizing instead to total heme c content results in a $k_{\text{cat}} = 5 \text{ e}^- \cdot \text{min}^{-1}$. For an evaluation of these numbers, see [Discussion](#).

Table 2. Activities of purified *TtcNOR* with different electron donors. Mean and standard deviation from measurements done in duplicates. For donors with $k_{\text{cat}} = 0$, no significant difference between sample and background could be detected. The activity was measured in 50 mM HEPES, pH 7.5, 50 mM KCl, 3 mM Asc, 0.05% DDM/GDN, at room temperature.

Sample	Electron donor	k_{cat} ($\text{e}^- \cdot \text{min}^{-1}$)
<i>TtcNOR</i> from <i>Tt</i> in DDM	Asc/TMPD (2.5 mM)	8 ± 3
	Asc/PMS (10 μM)	0
	Asc/TMPD (0.5 mM)/bovine cyt c (10 μM)	11 ± 9
	Asc/TMPD (0.5 mM)/cyt c_{552} (7.5 μM)	7 ± 4
	Asc/TMPD (0.5 mM)/NirM (7.5 μM)	0
<i>TtcNOR</i> from <i>Tt</i> in GDN	Asc/PMS (10 μM)	2 ± 1
<i>TtcNOR</i> from <i>Ec</i>	Asc/TMPD (2.5 mM)	3 ± 2

Table 3. NO-reducing activity in *Thermus thermophilus* HB27d-cNOR membranes, with activity in HB27d- ΔnorB subtracted. Mean and standard deviation from measurements done in duplicates. The activity was measured in 50 mM HEPES, pH 7.5, 50 mM KCl, and 3 mM Asc, at room temperature.

Electron donor	Activity ($\text{nM NO} \cdot \text{min}^{-1} \cdot \text{mg}^{-1}$)
Asc/TMPD (2.5 mM)	130 ± 30
Asc/PMS (10 μM)	140 ± 30

CO recombination

To compare ligand-binding properties of the active site in the different *TtcNOR*s, we studied CO recombination, a sensitive probe of the integrity of the active site. The rebinding of CO to the *TtcNOR* active site is biphasic, as previously observed for *PdcNOR* [27,44,54]. Example traces and difference spectra (reduced-CO bound minus reduced) are shown in Fig. 3. The difference spectra are qualitatively similar, differences observed are presumably due to contribution also of further reduction of the b_3 heme in the presence of CO. Comparison between *TtcNOR* expressed in *T. thermophilus* and in *E. coli* shows that the first phase has the same time constant ($t \sim 50 \mu\text{s}$ at 1 mM CO) in between the two preparations, whereas the slow phase is faster in the *E. coli* variant, see Table 4. Overall, both preparations have slower CO recombination than observed with *PdcNOR* (Table 4).

Table 4. Rate constants (k) and corresponding time constants ($\tau = 1/k$) obtained for CO recombination of *TtcNOR* from *Thermus thermophilus* (*Tt*) and *Escherichia coli* (*Ec*) at 100% and 20% CO.

Sample	k_{fast} ($\text{M}^{-1} \cdot \text{s}^{-1}$)	τ_{fast} (μs)	k_{slow} ($\text{M}^{-1} \cdot \text{s}^{-1}$)	τ_{slow} (ms)
<i>Tt</i> 100% (1 mM) CO	1.4×10^7	47	1.1×10^5	6.2
<i>Tt</i> 20% CO	2.0×10^7	170	2.5×10^5	13.5
<i>Ec</i> 100% CO	1.5×10^7	44	9.5×10^5	0.7
<i>Ec</i> 20%	1.9×10^7	174	1.4×10^6	2.4
<i>PdcNOR</i> 100% CO ^a	1.5×10^8	4	4.3×10^6	0.15
<i>PdcNOR</i> ΔnorQD 100% CO ^a	2.0×10^8	3	6.6×10^6	0.1

^aPreviously published values for *PdcNOR* at 100% CO with and without Fe_B (ΔnorQD) included for comparison.

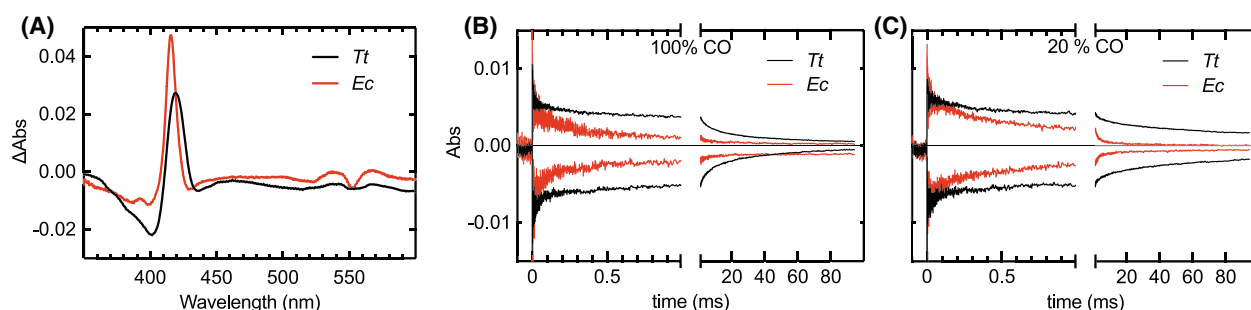


Fig. 3. CO binding and recombination in *TtcNOR*. (A) Difference spectra (reduced-CO bound minus reduced) of *TtcNOR* from *Thermus thermophilus* (black) and from *Escherichia coli* (red). Data was normalized to the absorbance at 420 nm in the reduced spectrum. (B, C) Traces from CO recombination with (B) 100% CO (1.5 mM) and (C) 20% CO (0.3 mM) followed at 415 nm (traces below zero) and 435 nm (traces above zero). *TtcNOR* expressed in *T. thermophilus* in black and in *E. coli* in red. Shown are averages of 20 traces, normalized to the same absorbance at 0.5 μs .

Sequence analysis

We wanted to investigate the prevalence of cNORs assembled in the absence of the *norQD* genes and if there are conserved features distinguishing them from NorQD-assisted cNORs. We focused on the cNORs analyzed in Ref. [45], where 259 NorB sequences were classified into nine different clades, based on sequence similarity. Of the 259 NorB sequences, 195 could be identified as having *norQ* and *norD* genes in proximity, 34 sequences as not having genes encoding the NorQD chaperones while 30 genomes could either not be found, or results were unclear (i.e., only one of the chaperone genes could be found or the genome was not annotated). Using the cNOR clades identified in Ref. [45], clades I–III and clades VIII and IX were almost exclusively cNOR with NorQD, while cNORs without NorQD dominate in clades IV–VII. Using multiple alignments, we identified several sequence differences between cNORs with and without NorQD. As already reported, *Ti*NorB lacks the two acidic surface residues (D220 and

E222 in *Pd*NorB) proposed to act as the binding site for NorD, conserved in cNORs with NorQD [28]. We can now show that (a) all 195 cNORs with NorQD chaperones have the conserved acidic residues D220 and E222 and (b) these are not conserved in cNORs without NorQD. Instead of the conserved acidic aspartate and glutamate, cNORs without NorQD have a variety of residues, for example proline, lysine, asparagine or glutamine (Fig. 4). Furthermore, we observe that among cNORs with NorQD, two conserved hydrophobic residues, found in the region corresponding to the K-pathway analog in qNOR (I244 and F290 in *Pac*-NOR), are exchanged for hydrophilic residues in cNORs lacking NorQD (Figs 4 and 5). For the full alignments and trees, see Figs S5–S7. We also made a smaller alignment of NorB and NorC sequences including also qNORs and the C-type HCuO as outgroup (Fig. 6), and we could see that NorB, as well as NorC sequences without chaperones cluster together, indicating co-evolution of the two subunits.

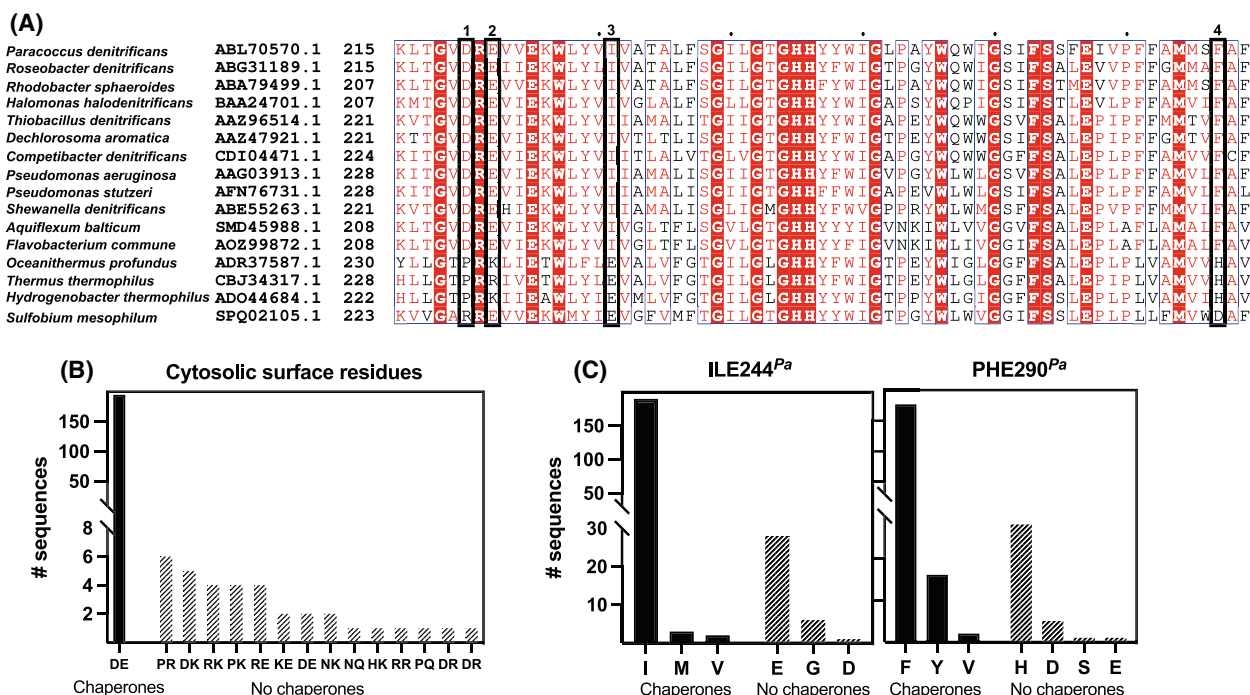


Fig. 4. (A) Alignment of a small selection of NorB sequences. (1) Acidic surface residue conserved D in cNORs with NorQD, not conserved in cNORs without NorQD. (2) The second acidic surface residue, conserved as E in cNORs with NorQD, not conserved in cNORs without NorQD. (3) K-analog pathway residue, conserved hydrophobic, mostly I, in cNORs with NorQD, less conserved but often E in cNORs without NorQD. (4) The second K-analog pathway residue, conserved aromatic, mostly F in cNORs with NorQD. Hydrophilic, often H, in cNORs without NorQD. For the full alignment with all sequences, see [Supporting Information](#). (B) Identity of NorB cytosolic surface residues (D220 and E222 in *Paracoccus denitrificans*) in all analyzed sequences. (C) Identity of channel residues (I244 and P290 in *Pseudomonas aeruginosa*) in all analyzed sequences.

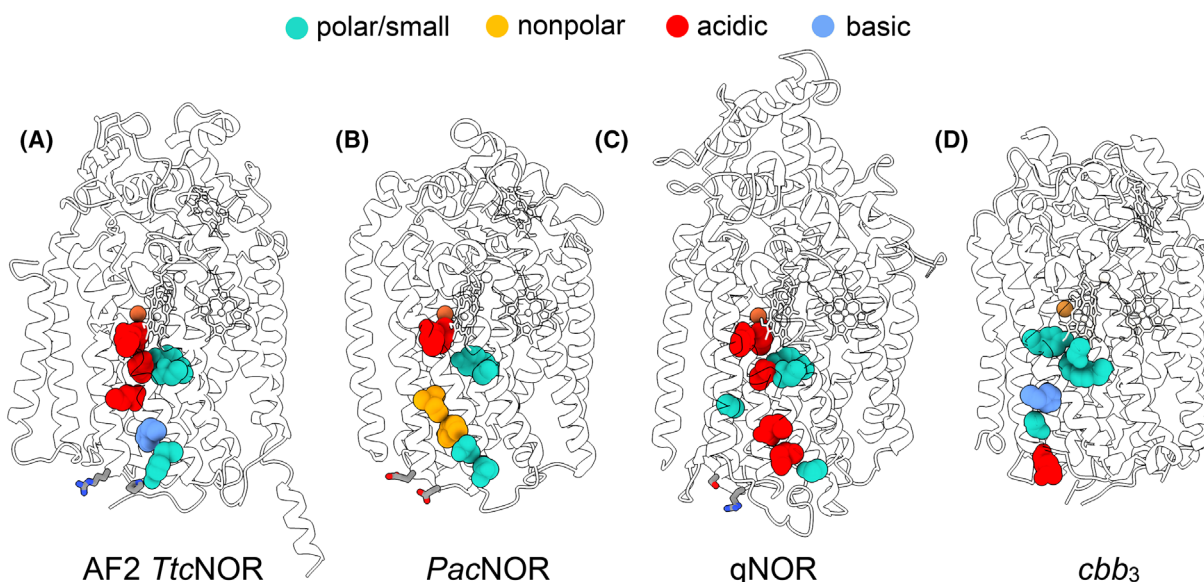


Fig. 5. Comparison of K-pathway analogues and cytosolic surface residues. (A) AlphaFold2 model of *Thermus thermophilus* cNOR, with NorH left out for clarity (full NorCBH depicted in Fig. S4). Ligands from *PacNOR* (PDB: 3O0R, [22]). (B) Crystal structure of *Pseudomonas aeruginosa* cNOR (PDB: 3O0R, [22]). (C) Cryo-EM structure of *Neisseria meningitidis* qNOR (PDB: 6L3h, [64]), shown as monomer (the enzyme forms a dimer, cf also Ref. [65]) for clarity. (D) Crystal structure of *Pseudomonas stutzeri* *cbb3*, with the third subunit CcoP left out for clarity (PDB: 3MK7, [71]). Overall structures, hemes and calcium ions are shown in white. Fe_B (NORs) and Cu_B (*cbb3*) are shown in orange and enlarged for clarity. Side chains of residues proposed to constitute the K-pathway analogues are shown in space fill and colored according to chemical properties: green for polar/small, yellow for nonpolar, red for acidic and blue for basic. Side chains of cytosolic surface residues are shown as sticks and enlarged for clarity.

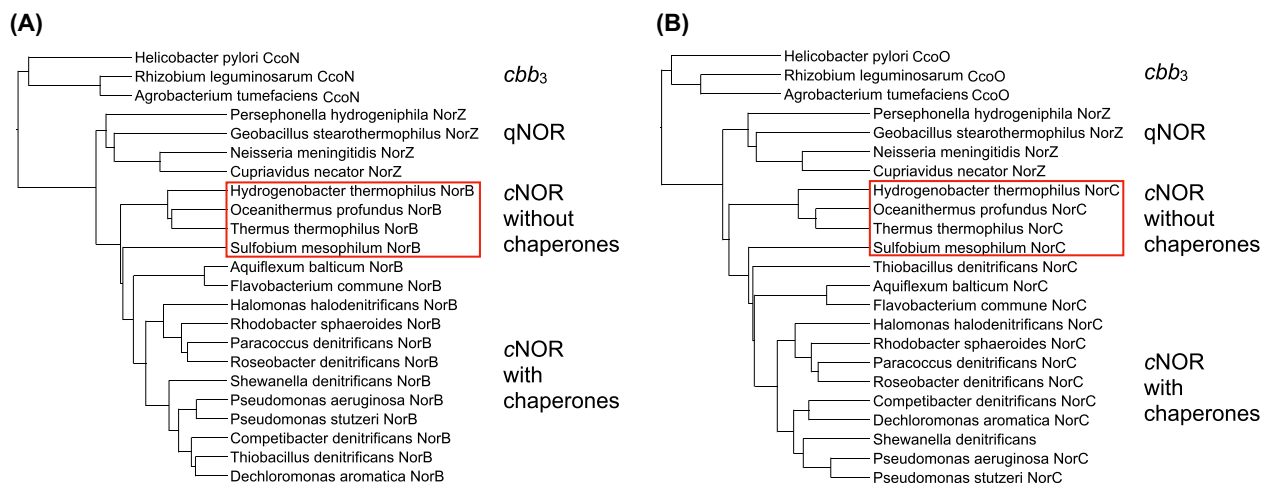


Fig. 6. (A) Phylogenetic tree of a small selection of NorB (with and without NorQD), NorZ (qNORs) and CcoN (*cbb3*) sequences. (B) Phylogenetic tree of a small selection of NorC (with and without NorQD), NorZ (qNOR) and CcoO (*cbb3*) sequences. For a full tree with all NorB sequences in our dataset, see Supporting Information.

Discussion

Catalytic activity of *TtcNOR*

The activity of *TtcNOR* is very low compared to previously characterized cNORs. The NO-reducing rates

we see in the natively expressed cNOR are similar to previous data on *TtcNOR* expressed homologously on an engineered vector in *T. thermophilus* and heterologously in *E. coli*, about 5–10 e⁻·min⁻¹ [30]. NirM, the putative native electron donor, here purified for the

first time, did not increase this activity. Furthermore, purified *Ttc*NOR does not exhibit the NOR characteristic substrate inhibition, with a maximum rate at about 5 μM NO [6]. The inhibition at higher [NO] is seen also for qNOR [24] and has been suggested to be due to NO binding to the oxidized μ -oxo bridged irons in the active site [10] and is sensitive to relative rates of reduction and oxidation of the active site [55]. It is also clear that when activity increases rather than decreases as [NO] goes down, there is no gradual loss of activity due to turnover-induced inactivation of the enzyme.

One can ask whether it is biologically relevant for an enzyme to reduce a couple of NO molecules per minute and question the need of a NOR, when *Ttcaa*₃ has higher NO-reducing activity [36]. Purified *Ttc*NOR activity has not been measured at *T. thermophilus* optimal growth temperature at $\sim 70^\circ\text{C}$, and most likely, it is more active at higher temperatures. However, temperature is probably not the only explanation, since the relatively high activity of *Ttcaa*₃ (30 min^{-1}) was measured at 20°C [36]. Our data indicates that the enzyme is more active in membranes than purified, with an activity of $\sim 130 \text{ nM NO} \cdot \text{min}^{-1} \cdot \text{mg}^{-1}$ membranes. Assuming that all cNOR present in the membranes could be purified, the activity in membranes is $\sim 600 \text{ e}^- \cdot \text{min}^{-1}$. If we instead normalize to total heme *c* content, the activity in membranes is $5 \text{ e}^- \cdot \text{min}^{-1}$. There are several heme *c* containing proteins putatively present in the *T. thermophilus* membranes, for example *caa*₃ [56,57], the *bc*₁ complex [58], and nitrate reductase (Nar) [33,59], of which at least the last one is expressed during denitrification [60]. Thus, the total heme *c* content is larger than the NorC content, implying that the activity in membranes probably is closer to $600 \text{ e}^- \cdot \text{min}^{-1}$ than to $5 \text{ e}^- \cdot \text{min}^{-1}$. In the membranes, we can also for the first time observe cNOR substrate inhibition, a good indicator of canonical cNOR activity. We suspected that the loss of activity could be due to harsh solubilization in DDM. Detergent solubilization can strip the membrane proteins of structurally and catalytically important lipids or break up protein complexes. It was previously shown that the nitrate reductase (Nar) complex in *T. thermophilus* harbors a membrane-bound *c* cytochrome suggested to enable the Nar to take over the role of the *bc*₁ complex during denitrification, and supply electrons to Nir and NOR [60]. It is possible that *Ttc*NOR receives electrons directly from this membrane-bound cyt *c*, or that it is part of a larger denitrifying supercomplex needed for stability and/or direct electron delivery. It could also be that structurally and/or catalytically important lipids are lost upon solubilization. Therefore, we also solubilized membranes in the milder detergent GDN. However, this

did not result in higher activity and we could not detect (by mass-spec) any co-purified denitrification components. Furthermore, the yield of *Ttc*NOR was much lower when solubilized in GDN, probably due to less efficient extraction from the membranes. We conclude that *Ttc*NOR is more active in its physiological membrane context, that the purification probably can be optimized further, and that the native electron donor is still not identified.

*Ttc*NOR was expressed in *E. coli* with two tags: an N-terminal histag on NorB and a C-terminal strep-tag on NorH. Pulling on NorB gave a *Ttc*NOR yield > 400 times higher than when pulling on NorH (Table S2). It seems that NorH either is not expressed or does not bind to cNOR when the enzyme is expressed in *E. coli*. NorH is not found in all cNORs lacking NorQD, but in a small subset of thermophilic bacteria. On the SDS/PAGE gel of the *E. coli* preparation, the NorB band is not visible upon boiling. Note however that the same pattern can be seen for *Pdc*NOR expressed in *E. coli*. Clearly, both the *Ttc*NOR and *Pdc*NOR expressed in *E. coli* have a lower resistance to high temperature than the natively expressed *Ttc*NOR.

We also investigated the ligand-binding properties of the *Ttc*NOR, using CO recombination, and compared between the natively expressed and the *E. coli* expressed *Ttc*NOR (that lacks the Fe_B, see below). In both preparations, CO recombination is overall slower than observed with the *Pdc*NOR [27], but the rapid component is still $> 10^7 \text{ M}^{-1} \cdot \text{s}^{-1}$. Interestingly, the rate constant for the fast phase is identical in the two preparations, whereas the slow phase is faster in the *E. coli* prep, see Table 4. This indicates that the active site is relatively intact and similar in at least a fraction of both preparations. Thus, the reason for the low activity of *Ttc*NOR is not due to a disturbed active site. Furthermore, this provides additional proof of Fe_B not being directly involved in CO binding, in line with previous results [27]. In *Pdc*NOR, there is essentially no difference in the rate constants of CO recombination between WT and Fe_B-less variants, however, the relative amplitude of the fast phase is small without Fe_B [27].

Metal insertion

We have previously shown that the NorQ and NorD proteins are essential for Fe_B insertion into *Pdc*NOR. NorQ, a MoxR AAA+ ATPase, and NorD, a VWA domain containing protein, form a complex that binds cNOR and uses ATP hydrolysis to fuel the Fe_B insertion process [27,28]. In this work, we wanted to investigate if and how the non-heme iron is inserted into a

cNOR lacking genes encoding NorQ and NorD; the *TtcNOR*. We observed that when *TtcNOR* is produced in *T. thermophilus* HB27 holding denitrifying genes from the denitrifying strain *T. thermophilus* PRQ25, the non-heme iron is inserted. However, when we produce *TtcNOR* heterologously in *E. coli*, transformed with the cNOR cluster (NorCBH), Fe_B is not present in the purified enzyme. Here, it should be noted that this is different from the previous study of *TtcNOR* expressed in *E. coli* where the total iron content was measured to 4 ± 0.25 Fe per enzyme, and mutating a conserved Fe_B binding glutamate (E211A) did not change the iron content [34]. However, the method of metal determination, measuring total iron content (including the three heme irons), was different from ours, measuring only non-heme iron. It is possible that the fourth iron found in Ref. [34] was bound somewhere other than the active site. We also note that this interpretation could explain why there was no change in the Fe_B-ligand mutant. Furthermore, one can argue that it is easier to distinguish between having or not having one non-heme iron, than it is to measure the difference between three and four total irons. However, the vector and growth conditions in the previous study was different from ours, and it is possible that Fe_B was retained in their preparation although it is not in ours. In our hands, Fe_B insertion is host dependent, but it is not clear why. Although the purity (A_{280}/A_{410}) of our samples varies between 1.3 and 2.5 (Table S2), none of the high scoring contaminants in the mass-spectrometry analysis (Table S3) of the natively expressed *TtcNOR* are iron containing proteins. Thus, the non-heme iron in our measurement should originate from the cNOR enzyme. As discussed below for qNOR, it is also possible that Fe_B is inserted into *TtcNOR* also in the *E. coli* membrane, but that it is lost during purification.

An obvious difference between the hosts *T. thermophilus* and *E. coli* is their difference in optimal growth temperature, and one could speculate that at high temperatures, there is a larger conformational flexibility and conformational changes leading to Fe_B insertion might not be ATP hydrolysis dependent. cNORs lacking Fe_B chaperones are found in several phyla, including thermophilic *Deinococcota* with the genera *Thermus* and *Oceanithermus* and the phylum *Aquificota*, with genus *Hydrogenobacter*, which all have species with cNORs lacking NorQD Fe_B chaperones. However, the lack of NorQD is not restricted to thermophilic bacteria; cNORs without NorQD in their gene cluster are also found in non-thermophilic species of several *Pseudomonadota* families (Figs S5 and S6). Many of these species are very little studied, and could

in principle have other, yet unknown chaperones for Fe_B insertion in cNOR. On the other hand, the genetics of *T. thermophilus* and its cNOR has been investigated thoroughly, and there are no reports on genes encoding NorQ or NorD in the NCE nor in the *nir-nor* cluster [29,33]. *T. thermophilus* does encode other MoxR AAA+ ATPases, for example RavA (Uniprot A0A3P4ATT4), proposed to be associated with fumarate reductase [61,62]. Thus, *T. thermophilus* does make use of MoxR chaperone-dependent processes, just not for Fe_B insertion in cNOR.

The second most studied NOR, qNOR, is, just like *TtcNOR*, independent on chaperone proteins for non-heme iron insertion. qNOR is a one-subunit enzyme and has only the corresponding gene (*norZ*) in its gene cluster. qNOR has a water-filled pathway lined by hydrophilic and/or protonatable amino acids, leading from the cytosol to the active site [24,25,63–65], suggested to function as a channel for substrate protons [24,25]. The channel, called the K-analog after its similarity in location (but not in amino acid conservation) with the K-pathway for protons in A- (B- and C-type) O₂-reducing HCuOs, could perhaps in addition to (or instead of) proton transfer, enable iron insertion without chaperones. This could be done by directly providing access to iron ions, but also in a more indirect way by leading to a different folding/assembly pathway involving higher bulk access. As previously discussed in Ref. [66], the K-analog is ‘plugged’ by hydrophobic residues in many cNORs, but not in qNOR, nor in *TtcNOR* (see Fig. 6). We used alignments of NorB sequences connected or not to NorQD to investigate the possible correlation between having an open K-analog and lack of NorQD chaperones (Fig. 4). Throughout the whole dataset, cNORs with NorQD have hydrophobic residues plugging the K-analog, and in cNORs without NorQD, those residues are hydrophilic, leaving the K-analog open. Thus, the need for chaperones seems to be determined by (or at least correlated with) the state of the K-analog. Previous data suggest that qNORs might be electrogenic due to the ability to take up substrate protons from the cytoplasm [24], in contrast to cNORs, acquiring protons from the periplasm.

It should be noted that the notion of a K-pathway analogue in qNORs has been challenged based on the lack of detailed conserved sequence patterns [4]. However, there are NORs with conserved K-pathway analogues, the Cu_ANORs [67,68], related to the B-type HCuOs instead of the C-type (as for *c* and qNOR). Cu_ANORs have a K-pathway analogue with a conserved sequence pattern [4], and were shown to be electrogenic [68]. The Cu_ANOR does not have the NorQD

chaperones in their gene cluster. Thus, cNORs with an open K-analog could in theory be electrogenic, and in some cNORs, at some point in evolution, the ability to contribute to the electrochemical gradient was lost. In addition, Fe_B insertion in cNORs without the K-analog is ATP dependent, making the closing of the channel even more energetically disadvantageous. This raises the question, why close the pathway?

In the first crystal structure of qNOR [25], the *Geobacillus stearothermophilus* (Gs) enzyme was produced in *E. coli* and the structure revealed a zinc ion in the active site, instead of Fe_B. In the same study, they showed that GsqNOR from the native host or from *E. coli* but prepared with the detergent DDM, instead of the *n*-octyl-β-D-glucoside (βOG) detergent used for crystallization, contained fractions with either Fe_B or Zn_B. Thus, the metal content depended on solubilization, indicating that the Fe_B in qNOR can be lost, and replaced by alternative metals, such as zinc. On the other hand, qNOR from *Ralstonia eutropha* [69] and *Pyrobaculum aerophilum* [70] expressed in their native hosts (as well as the *Neisseria meningitidis* qNOR expressed in *E. coli* [24]) were shown to have the non-heme iron. These results, and the results in this work, indicates that integrity and metal content of the active site in NORs can be both preparation dependent and host dependent. Perhaps un-assisted uptake of iron through the K-analog is less tightly regulated and more easily leads to incorporation of or exchange for the incorrect metal, compared to the chaperone-mediated insertion in for example *PdcNOR*. When

PdcNOR is expressed heterologously without chaperones, the Fe_B site was previously shown to be empty, and not occupied by any alternative metal [27].

The observation that some cNORs lack chaperones for metal insertion provides an additional clue on the evolution of NORs, see Fig. 7. Hydrophilic channels leading from the cytoplasm to the active site are found in C-type O₂-reducing HCuOs, qNORs and perhaps in certain cNORs. The rooting of the phylogenetic tree of HCuOs is highly debated [4,66,71] and it is not known whether the first HCuO was O₂- or NO-reducing. However, (q and c) NORs are clearly more closely related to the C-type oxidases than to the A- and B-type. We will focus on the evolutionary relationship between NORs and C-type oxidases, and root the tree in an electrogenic HCuO with an open K-pathway and an ambiguous preferred substrate (O₂ or NO) (Fig. 7). It is likely that the closing of the channel and the concomitant ‘invention’ of NorQD chaperones in cNORs happened after the branching between cNORs and qNORs, and that *TtcNORs* and other cNORs without NorQD branched off before closing the channel. It is also possible that cNORs without NorQD (like *TtcNOR*) constitute the root. Closing the channel and relying on ATP-dependent metal insertion could be more advantageous in certain environments, for example where the iron supply is low, and a lost iron would be hard to replace. In addition, as cNORs with a closed K-pathway (and hence relying on NorQD for iron insertion) were found to occur more often in (high-potential) ubiquinol, rather than (low potential)

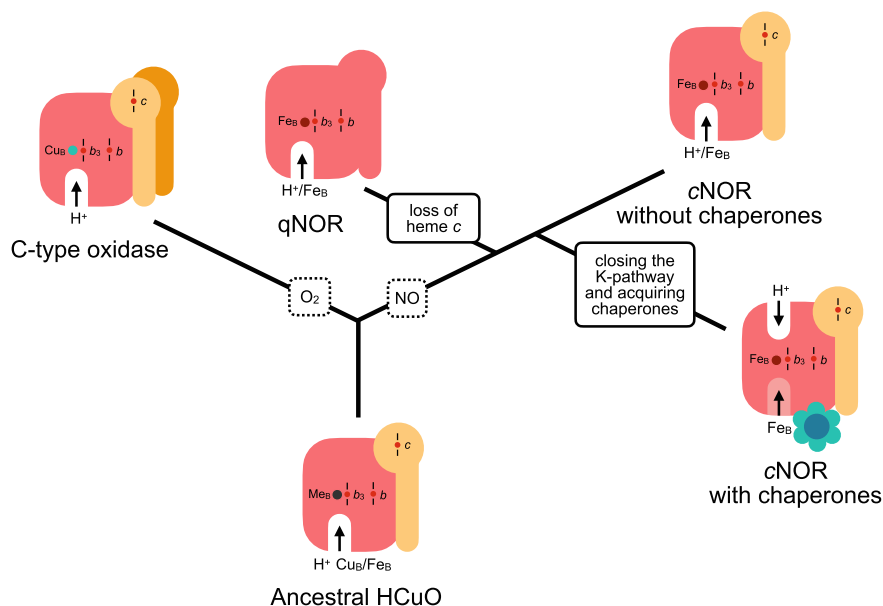


Fig. 7. Hypothetical scenario of the evolution of C-type oxidases and related NORs, with evolutionary events marked out in boxes.

menaquinol-using organisms [66], and the cyt *c* pool, reduced by the bc₁-complex, is oxidized through several paths, it could have been a thermodynamic ‘compromise’ to lose the electrogenicity of the NO-reducing reaction in order to achieve reliable flow through the denitrification chain.

Conclusions

TtcNOR is an example of a cNOR lacking chaperones NorQD for insertion of the non-heme iron. In this work, we have shown that Fe_B insertion occurs without the chaperones when the enzyme is produced in its native host, but not in *E. coli*. We also show that the catalytic activity is low in all purified *TtcNOR* samples, independent on whether Fe_B is inserted or not, and we show that NO reduction is likely to be more efficient in intact *T. thermophilus* membranes. Furthermore, we propose that the insertion of Fe_B without chaperones in certain cNORs, and in qNOR, is enabled by a hydrophilic channel leading from the cytosol to the active site, and that ‘plugging’ of this hydrophilic channel in e.g., the *Paracoccus denitrificans* cNOR led to the need for using chaperone-assisted Fe_B insertion and is a relatively late evolutionary event.

Acknowledgements

This work was supported by The Swedish Research Council (VR, nr. 2019-04124). We are grateful to José Berenguer (Universidad Autonoma de Madrid) for providing us with the modified *T. thermophilus* HB27d strains, the pMK-cNOR plasmid and advice on growing them. We also want to thank Christoph von Ballmoos (University of Bern) and Ferdinand Greiss (Weizmann Institute) for the cyt *c*₅₅₂-his plasmid, and Molly Foley and Dylan Thomas from the student exchange with University of Illinois for their contribution to the growing of *T. thermophilus* and the expression of the NirM protein, respectively.

Author contributions

SA and PÄ designed the study, SA performed all experiments, SA and PÄ analyzed data, SA wrote the original manuscript draft, SA and PÄ revised the manuscript.

Peer review

The peer review history for this article is available at <https://www.webofscience.com/api/gateway/wos/peer-review/10.1002/1873-3468.70007>.

Data accessibility

The data generated and analyzed during this study are included in the published article and its [Supporting Information](#). Additional data is available from the corresponding author upon reasonable request.

References

- 1 Ravishankara A, Daniel JS and Portmann RW (2009) Nitrous oxide (N₂O): the dominant ozone-depleting substance emitted in the 21st century. *Science* **326**, 123–125.
- 2 Hedlund BP, McDonald AI, Lam J, Dodsworth JA, Brown JR and Hungate BA (2011) Potential role of *Thermus thermophilus* and *T. oshimai* in high rates of nitrous oxide (N₂O) production in ~80°C hot springs in the US Great Basin. *Geobiology* **9**, 471–480.
- 3 Sousa FL, Alves RJ, Pereira-Leal JB, Teixeira M and Pereira MM (2011) A bioinformatics classifier and database for heme-copper oxygen reductases. *PLoS One* **6**, e19117.
- 4 Murali R, Pace LA, Sanford RA, Ward LM, Lynes MM, Hatzenpichler R, Lingappa UF, Fischer WW, Gennis RB and Hemp J (2024) Diversity and evolution of nitric oxide reduction in bacteria and archaea. *Proc Natl Acad Sci USA* **121**, e2316422121.
- 5 Hendriks JH, Jasaitis A, Saraste M and Verkhovsky MI (2002) Proton and electron pathways in the bacterial nitric oxide reductase. *Biochemistry* **41**, 2331–2340.
- 6 Girsch P and de Vries S (1997) Purification and initial kinetic and spectroscopic characterization of NO reductase from *Paracoccus denitrificans*. *Biochim Biophys Acta* **1318**, 202–216.
- 7 Zumft WG (2005) Nitric oxide reductases of prokaryotes with emphasis on the respiratory, heme–copper oxidase type. *J Inorg Biochem* **99**, 194–215.
- 8 Moënné-Loccoz P and De Vries S (1998) Structural characterization of the catalytic high-spin heme b of nitric oxide reductase: a resonance Raman study. *J Am Chem Soc* **120**, 5147–5152.
- 9 Kumita H, Matsuura K, Hino T, Takahashi S, Hori H, Fukumori Y, Morishima I and Shiro Y (2004) NO reduction by nitric-oxide reductase from denitrifying bacterium *Pseudomonas aeruginosa*: characterization of reaction intermediates that appear in the single turnover cycle. *J Biol Chem* **279**, 55247–55254.
- 10 Blomberg MR and Siegbahn PE (2012) Mechanism for N₂O generation in bacterial nitric oxide reductase: a quantum chemical study. *Biochemistry* **51**, 5173–5186.
- 11 Takeda H, Kimura T, Nomura T, Horitani M, Yokota A, Matsubayashi A, Ishii S, Shiro Y, Kubo M and Tosha T (2020) Timing of NO binding and protonation in the catalytic reaction of bacterial nitric oxide

- reductase as established by time-resolved spectroscopy. *Bull Chem Soc Jpn* **93**, 825–833.
- 12 Lachmann P, Huang Y, Reimann J, Flock U and Ädelroth P (2010) Substrate control of internal electron transfer in bacterial nitric-oxide reductase. *J Biol Chem* **285**, 25531–25537.
- 13 Heiss B, Frunzke K and Zumft W (1989) Formation of the NN bond from nitric oxide by a membrane-bound cytochrome bc complex of nitrate-respiring (denitrifying) *Pseudomonas stutzeri*. *J Bacteriol* **171**, 3288–3297.
- 14 Kastrau DH, Heiss B, Kroneck PM and Zumft WG (1994) Nitric oxide reductase from *Pseudomonas stutzeri*, a novel cytochrome bc complex: phospholipid requirement, electron paramagnetic resonance and redox properties. *Eur J Biochem* **222**, 293–303.
- 15 Hoglen J and Hollocher T (1989) Purification and some characteristics of nitric oxide reductase-containing vesicles from *Paracoccus denitrificans*. *J Biol Chem* **264**, 7556–7563.
- 16 Carr GJ and Ferguson SJ (1990) The nitric oxide reductase of *Paracoccus denitrificans*. *Biochem J* **269**, 423–429.
- 17 Sakurai N and Sakurai T (1998) Genomic DNA cloning of the region encoding nitric oxide reductase in *Paracoccus halodenitrificans* and a structure model relevant to cytochrome oxidase. *Biochem Biophys Res Commun* **243**, 400–406.
- 18 Sakurai T, Nakashima S, Kataoka K, Seo D and Sakurai N (2005) Diverse NO reduction by *Halomonas halodenitrificans* nitric oxide reductase. *Biochem Biophys Res Commun* **333**, 483–487.
- 19 Matsuda Y, Inamori K, Osaki T, Eguchi A, Watanabe A, Kawabata S, Iba K and Arata H (2002) Nitric oxide-reductase homologue that contains a copper atom and has cytochrome c-oxidase activity from an aerobic phototrophic bacterium *Roseobacter denitrificans*. *J Biochem* **131**, 791–800.
- 20 Crow A, Matsuda Y, Arata H and Oubrie A (2016) Structure of the membrane-intrinsic nitric oxide reductase from *Roseobacter denitrificans*. *Biochemistry* **55**, 3198–3203.
- 21 Matsuda Y, Uchida T, Hori H, Kitagawa T and Arata H (2004) Structural characterization of a binuclear center of a Cu-containing NO reductase homologue from *Roseobacter denitrificans*: EPR and resonance Raman studies. *Biochim Biophys Acta* **1656**, 37–45.
- 22 Hino T, Matsumoto Y, Nagano S, Sugimoto H, Fukumori Y, Murata T, Iwata S and Shiro Y (2010) Structural basis of biological N₂O generation by bacterial nitric oxide reductase. *Science* **330**, 1666–1670.
- 23 Reimann J, Flock U, Lepp H, Honigsmann A and Ädelroth P (2007) A pathway for protons in nitric oxide reductase from *Paracoccus denitrificans*. *Biochim Biophys Acta* **1767**, 362–373.
- 24 Gonska N, Young D, Yuki R, Okamoto T, Hisano T, Antonyuk S, Hasnain SS, Muramoto K, Shiro Y, Tosha T *et al.* (2018) Characterization of the quinol-dependent nitric oxide reductase from the pathogen *Neisseria meningitidis*, an electrogenic enzyme. *Sci Rep* **8**, 3637.
- 25 Matsumoto Y, Tosha T, Pislakov AV, Hino T, Sugimoto H, Nagano S, Sugita Y and Shiro Y (2012) Crystal structure of quinol-dependent nitric oxide reductase from *Geobacillus stearothermophilus*. *Nat Struct Mol Biol* **19**, 238–245.
- 26 Shiro Y (2012) Structure and function of bacterial nitric oxide reductases: nitric oxide reductase, anaerobic enzymes. *Biochim Biophys Acta* **1817**, 1907–1913.
- 27 Kahle M, ter Beek J, Hosler JP and Ädelroth P (2018) The insertion of the non-heme FeB cofactor into nitric oxide reductase from *P. denitrificans* depends on NorQ and NorD accessory proteins. *Biochim Biophys Acta* **1859**, 1051–1058.
- 28 Kahle M, Appelgren S, Elofsson A, Carroni M and Ädelroth P (2023) Insights into the structure-function relationship of the NorQ/NorD chaperones from *Paracoccus denitrificans* reveal shared principles of interacting MoxR AAA+/VWA domain proteins. *BMC Biol* **21**, 47.
- 29 Alvarez L, Bricio C, Gómez MJ and Berenguer J (2011) Lateral transfer of the denitrification pathway genes among *Thermus thermophilus* strains. *Appl Environ Microbiol* **77**, 1352–1358.
- 30 Bricio C, Alvarez L, San Martin M, Schurig-Briccio LA, Gennis RB and Berenguer J (2014) A third subunit in ancestral cytochrome c-dependent nitric oxide reductases. *Appl Environ Microbiol* **80**, 4871–4878.
- 31 Ramírez-Arcos S, Fernández-Herrero LA, Marín I and Berenguer J (1998) Anaerobic growth, a property horizontally transferred by an Hfr-like mechanism among extreme thermophiles. *J Bacteriol* **180**, 3137–3143.
- 32 Ramírez-Arcos S, Fernández-Herrero LA and Berenguer J (1998) A thermophilic nitrate reductase is responsible for the strain specific anaerobic growth of *Thermus thermophilus* HB8. *Biochim Biophys Acta* **1396**, 215–227.
- 33 Alvarez L, Bricio C, Blesa A, Hidalgo A and Berenguer J (2014) Transferable denitrification capability of *Thermus thermophilus*. *Appl Environ Microbiol* **80**, 19–28.
- 34 Schurig-Briccio LA, Venkatakrishnan P, Hemp J, Bricio C, Berenguer J and Gennis RB (2013) Characterization of the nitric oxide reductase from *Thermus thermophilus*. *Proc Natl Acad Sci USA* **110**, 12613–12618.
- 35 Thorndycroft FH, Butland G, Richardson DJ and Watmough NJ (2007) A new assay for nitric oxide reductase reveals two conserved glutamate residues

- form the entrance to a proton-conducting channel in the bacterial enzyme. *Biochem J* **401**, 111–119.
- 36 Giuffrè A, Stubauer G, Sarti P, Brunori M, Zumft WG, Buse G and Soulimane T (1999) The heme-copper oxidases of *Thermus thermophilus* catalyze the reduction of nitric oxide: evolutionary implications. *Proc Natl Acad Sci USA* **96**, 14718–14723.
 - 37 Fee JA, Chen Y, Todaro TR, Bren KL, Patel KM, Hill MG, Gomez-Moran E, Loehr TM, Ai J, Thöny-meyer L *et al.* (2000) Integrity of *Thermus thermophilus* cytochrome c552 synthesized by *Escherichia coli* cells expressing the host-specific cytochrome c maturation genes, ccmABCDEFGH: biochemical, spectral, and structural characterization of the recombinant protein. *Protein Sci* **9**, 2074–2084.
 - 38 Keightley JA, Sanders D, Todaro TR, Pastuszyn A and Fee JA (1998) Cloning and expression in *Escherichia coli* of the cytochrome c 552 gene from *Thermus thermophilus* HB8: evidence for genetic linkage to an ATP-binding cassette protein and initial characterization of the cycA gene products. *J Biol Chem* **273**, 12006–12016.
 - 39 Arslan E, Schulz H, Zufferey R, Künzler P and Thöny-Meyer L (1998) Overproduction of the *Bradyrhizobium japonicum* c-type cytochrome subunits of the cbb3 oxidase in *Escherichia coli*. *Biochem Biophys Res Commun* **251**, 744–747.
 - 40 Zhang Z, Kuipers G, Niemiec Ł, Baumgarten T, Slotboom DJ, de Gier JW and Hjelm A (2015) High-level production of membrane proteins in *E. coli* BL21 (DE3) by omitting the inducer IPTG. *Microb Cell Fact* **14**, 1–11.
 - 41 Flock U, Thorndycroft FH, Matorin AD, Richardson DJ, Watmough NJ and Ädelroth P (2008) Defining the proton entry point in the bacterial respiratory nitric-oxide reductase. *J Biol Chem* **283**, 3839–3845.
 - 42 Hennessy DJ, Reid GR, Smith FE and Thompson SL (1984) Ferene—a new spectrophotometric reagent for iron. *Can J Chem* **62**, 721–724.
 - 43 Pierik AJ, Wolbert RB, Mutsaers PH, Hagen WR and Veeger C (1992) Purification and biochemical characterization of a putative [6Fe-6S] prismatic-cluster-containing protein from *Desulfovibrio vulgaris* (Hildenborough). *Eur J Biochem* **206**, 697–704.
 - 44 Flock U, Watmough NJ and Ädelroth P (2005) Electron/proton coupling in bacterial nitric oxide reductase during reduction of oxygen. *Biochemistry* **44**, 10711–10719.
 - 45 Woo S-G, Sewell HL and Criddle CS (2022) Phylogenetic diversity of NO reductases, new tools for nor monitoring, and insights into N₂O production in natural and engineered environments. *Front Environ Sci Eng* **16**, 127.
 - 46 Wheeler DL, Barrett T, Benson DA, Bryant SH, Canese K, Chetvernin V, Church DM, DiCuccio M, Edgar R, Federhen S *et al.* (2007) Database resources of the national center for biotechnology information. *Nucleic Acids Res* **36**(Suppl 1), D13–D21.
 - 47 Sievers F, Wilm A, Dineen D, Gibson TJ, Karplus K, Li W, Lopez R, McWilliam H, Remmert M, Söding J *et al.* (2011) Fast, scalable generation of high-quality protein multiple sequence alignments using Clustal Omega. *Mol Syst Biol* **7**, 539.
 - 48 Robert X and Gouet P (2014) Deciphering key features in protein structures with the new ENDscript server. *Nucleic Acids Res* **42**, W320–W324.
 - 49 Jumper J, Evans R, Pritzel A, Green T, Figurnov M, Ronneberger O, Tunyasuvunakool K, Bates R, Židek A, Potapenko A *et al.* (2021) Highly accurate protein structure prediction with AlphaFold. *Nature* **596**, 583–589.
 - 50 Evans R, O'Neill M, Pritzel A, Antropova N, Senior A, Green T, Židek A, Bates R, Blackwell S, Yim J *et al.* (2021) Protein complex prediction with AlphaFold-Multimer. *bioRxiv*. doi: [10.1101/2021.10.04.463034](https://doi.org/10.1101/2021.10.04.463034)
 - 51 Mirdita M, Schütze K, Moriwaki Y, Heo L, Ovchinnikov S and Steinegger M (2022) ColabFold: making protein folding accessible to all. *Nat Methods* **19**, 679–682.
 - 52 Pettersen EF, Goddard TD, Huang CC, Meng EC, Couch GS, Croll TI, Morris JH and Ferrin TE (2021) UCSF ChimeraX: structure visualization for researchers, educators, and developers. *Protein Sci* **30**, 70–82.
 - 53 Moe A, Di Trani J, Rubinstein JL and Brzezinski P (2021) Cryo-EM structure and kinetics reveal electron transfer by 2D diffusion of cytochrome c in the yeast III-IV respiratory supercomplex. *Proc Natl Acad Sci USA* **118**, e2021157118.
 - 54 Hendriks JH, Prior L, Baker AR, Thomson AJ, Saraste M and Watmough NJ (2001) Reaction of carbon monoxide with the reduced active site of bacterial nitric oxide reductase. *Biochemistry* **40**, 13361–13369.
 - 55 Koutný M and Kučera I (1999) Kinetic analysis of substrate inhibition in nitric oxide reductase of *Paracoccus denitrificans*. *Biochem Biophys Res Commun* **262**, 562–564.
 - 56 Fee JA, Choc MG, Findling KL, Lorence R and Yoshida T (1980) Properties of a copper-containing cytochrome claa3 complex: a terminal oxidase of the extreme thermophile *Thermus thermophilus* HB8. *Proc Natl Acad Sci USA* **77**, 147–151.
 - 57 Hon-nami K and Oshima T (1980) Cytochrome oxidase from an extreme thermophile, *Thermus thermophilus* HB 8. *Biochem Biophys Res Commun* **92**, 1023–1029.
 - 58 Mooser D, Maneg O, Corvey C, Steiner T, Malatesta F, Karas M, Soulimane T and Ludwig B (2005) A four-subunit cytochrome bc₁ complex complements the respiratory chain of *Thermus thermophilus*. *Biochim Biophys Acta* **1708**, 262–274.

- 59 Zafra O, Cava F, Blasco F, Magalon A and Berenguer J (2005) Membrane-associated maturation of the heterotetrameric nitrate reductase of *Thermus thermophilus*. *J Bacteriol* **187**, 3990–3996.
- 60 Cava F, Zafra O and Berenguer J (2008) A cytochrome c containing nitrate reductase plays a role in electron transport for denitrification in *Thermus thermophilus* without involvement of the bc respiratory complex. *Mol Microbiol* **70**, 507–518.
- 61 Wong KS, Bhandari V, Janga SC and Houry WA (2017) The RavA-ViaA chaperone-like system interacts with and modulates the activity of the fumarate reductase respiratory complex. *J Mol Biol* **429**, 324–344.
- 62 Wong KS, Snider JD, Graham C, Greenblatt JF, Emili A, Babu M and Houry WA (2014) The MoxR ATPase RavA and its cofactor ViaA interact with the NADH: ubiquinone oxidoreductase I in *Escherichia coli*. *PLoS One* **9**, e85529.
- 63 Gopalasingam CC, Johnson RM, Chiduzu GN, Tosha T, Yamamoto M, Shiro Y, Antonyuk SV, Muench SP and Hasnain SS (2019) Dimeric structures of quinol-dependent nitric oxide reductases (qNORs) revealed by cryo-electron microscopy. *Sci Adv* **5**, eaax1803.
- 64 Jamali MAM, Gopalasingam CC, Johnson RM, Tosha T, Muramoto K, Muench SP, Antonyuk SV, Shiro Y and Hasnain SS (2020) The active form of quinol-dependent nitric oxide reductase from *Neisseria meningitidis* is a dimer. *IUCrJ* **7**, 404–415.
- 65 Flynn AJ, Antonyuk SV, Eady RR, Muench SP and Hasnain SS (2023) A 2.2 Å cryoEM structure of a quinol-dependent NO reductase shows close similarity to respiratory oxidases. *Nat Commun* **14**, 3416.
- 66 Ducluzeau A-L, Schoepp-Cothenet B, van Lis R, Baymann F, Russell MJ and Nitschke W (2014) The evolution of respiratory O₂/NO reductases: an out-of-the-phylogenetic-box perspective. *J R Soc Interface* **11**, 20140196.
- 67 Suharti, Strampraad MJ, Schröder I and de Vries S (2001) A novel copper a containing menaquinol NO reductase from *Bacillus azotoformans*. *Biochemistry* **40**, 2632–2639.
- 68 Al-Attar S and de Vries S (2015) An electrogenic nitric oxide reductase. *FEBS Lett* **589**, 2050–2057.
- 69 Cramm R, Pohlmann A and Friedrich B (1999) Purification and characterization of the single-component nitric oxide reductase from *Ralstonia eutropha* H16. *FEBS Lett* **460**, 6–10.
- 70 de Vries S, Strampraad MJ, Lu S, Moënné-Loccoz P and Schröder I (2003) Purification and characterization of the MQH2: NO oxidoreductase from the hyperthermophilic archaeon *Pyrobaculum aerophilum*. *J Biol Chem* **278**, 35861–35868.
- 71 Gribaldo S, Talla E and Brochier-Armanet C (2009) Evolution of the haem copper oxidases superfamily: a rooting tale. *Trends Biochem Sci* **34**, 375–381.

Supporting information

Additional supporting information may be found online in the Supporting Information section at the end of the article.

Fig. S1. Sequence for expression of NirM, codon optimized for *Escherichia coli*.

Fig. S2. SDS/PAGE of cyt *c*₅₅₂ and NirM and corresponding spectra.

Fig. S3. Original gels for Fig. 1D and Fig. S2.

Fig. S4. AlphaFold model of NorBCH TtcNOR.

Fig. S5. Multiple sequence alignment of *norB* sequences, part 1.

Fig. S6. Multiple sequence alignment of *norB* sequences, part 2.

Fig. S7. Phylogenetic tree of aligned *norB* sequences.

Table S1. Primers for amplification of the cNOR gene cluster.

Table S2. Yields, purity and absorbance peaks of protein preparations.

Table S3. Mass-spectroscopy results.